Direct detection of H atoms in the catalytic chemical vapor deposition of the SiH_4/H_2 system

Hironobu Umemoto,[a] Kentaro Ohara, and Daisuke Morita
School of Materials Science, Japan Advanced Institute of Science and Technology, Asahidai, Tatsunokuchi, Nomi, Ishikawa 923-1292, Japan

Yoshitaka Nozaki
School of Materials Science, Japan Advanced Institute of Science and Technology, Asahidai, Tatsunokuchi, Nomi, Ishikawa 923-1292, Japan and Sigma Koki Co., Ltd., Yazukaho, Matto, Ishikawa 924-0838, Japan

Atsushi Masuda and Hideki Matsumura
School of Materials Science, Japan Advanced Institute of Science and Technology, Asahidai, Tatsunokuchi, Nomi, Ishikawa 923-1292, Japan

(Received 30 July 2001; accepted for publication 26 October 2001)

The absolute densities of H atoms produced in catalytic chemical vapor deposition (Cat-CVD or hot-wire CVD) processes were determined by employing two-photon laser-induced fluorescence and vacuum ultraviolet absorption techniques. The H-atom density in the gas phase increases exponentially with increases in the catalyzer temperature in the presence of pure H_2. When the catalyzer temperature was 2200 K, the absolute density in the presence of 5.6 Pa of H_2 (150 sccm in flow rate) was as high as 1.5×10^{14} cm^{-3} at a point 10 cm from the catalyzer. This density is one or two orders of magnitude higher than those observed in typical plasma-enhanced chemical vapor-deposition processes. The H-atom density decreases sharply with the addition of SiH_4. When 0.1 Pa of SiH_4 was added, the steady-state density decreased to 7×10^{12} cm^{-3}. This sharp decrease can primarily be ascribed to the loss processes on chamber walls. © *2002 American Institute of Physics.* [DOI: 10.1063/1.1428800]

I. INTRODUCTION

Catalytic chemical vapor deposition (Cat-CVD), often called hot-wire chemical vapor deposition, is one of the most promising techniques for producing semiconductor thin films at low temperatures.[1–5] Device-quality amorphous silicon, polycrystalline silicon, and silicon nitride films are easily obtained at substrate temperatures as low as 600 K. In this technique, gaseous materials, such as SiH_4 and H_2, are introduced into a vacuum chamber where they decompose into radical species upon contact with heated catalyzer surfaces.

The identification of radical species produced on catalyzer surfaces as well as an understanding of the fundamental kinetics of this process in the gas phase are essential in designing the chemical vapor deposition (CVD) apparatus and in optimization of deposition conditions. Based on the results of laser spectroscopic measurements, we have recently reported that one of the major products in the cracking reaction of SiH_4 on heated tungsten surfaces is atomic silicon.[6] The direct production of SiH and SiH_3 radicals is found to be minor.[6,7] These observations are consistent with the results of other mass spectrometric measurements.[3,8,9] When collisional processes in the gas phase can be ignored, Si atoms should be deposited directly on the substrate surfaces. Under practical deposition conditions, however, chemical reactions in the gas phase do play an important role. For example, H-atoms are expected to be produced efficiently from H_2 on heated catalyzer surfaces,[10,11] and react with SiH_4 to produce SiH_3.[12–14] We have succeeded in detecting SiH_3 in a H_2/SiH_4 system by using a cavity ringdown technique and have shown that SiH_3 is one of the strongest candidates for the film precursor under practical conditions.[7] The steady-state density of SiH_3 in the presence of 5.6 Pa of H_2 and 1.0 Pa of SiH_4 is 1.0×10^{12} cm^{-3}. This density is two orders of magnitude larger than that of Si atoms under identical conditions.

Although the existence of SiH_3 strongly suggests the importance of the $H+SiH_4$ reaction in the gas phase, direct detection of H-atoms is essential for further discussion. H-atoms are also important in the etching of silicon compounds on surfaces.[6,15–17] In the present work, the absolute densities of H-atoms were determined under various conditions by employing laser spectroscopic techniques.

II. EXPERIMENT

The CVD chamber and other experimental apparatus were similar to those described previously for the detection of Si, SiH, and SiH_3.[6,7] The length and diameter of the catalyzer (W wire) were 120 cm and 0.4 mm, respectively. The detection zone was 10 cm below the catalyzer and 5 cm above the substrate holder. The substrate holder was not heated in the present measurements. The absolute densities

[a]Author to whom correspondence should be addressed; electronic mail: umemoto@jaist.ac.jp

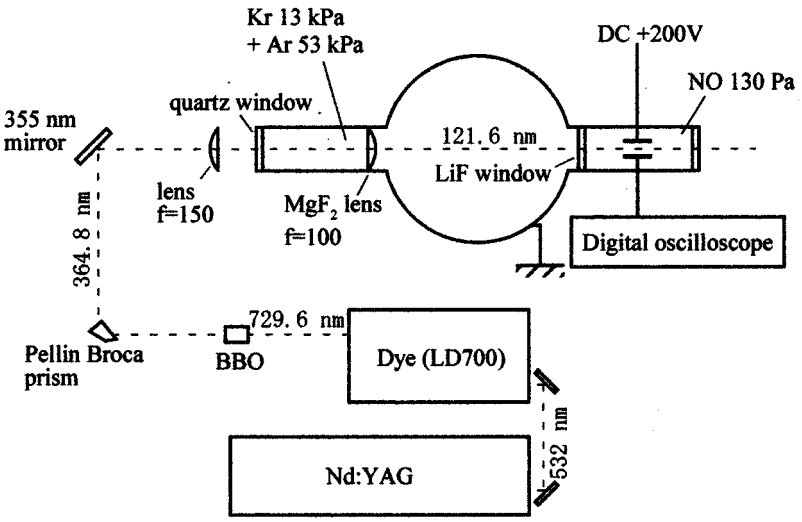

FIG. 1. Schematic diagram of the experimental apparatus for the vacuum ultraviolet absorption measurements.

of H-atoms in the gas phase were determined by combining a two-photon laser-induced fluorescence (LIF) technique[18] and a vacuum ultraviolet (Lyman α) absorption technique. The principle of the present procedure is the same as that employed by Tachibana,[19] except that a laser was used as the vacuum ultraviolet light source. The absolute densities of H atoms can be determined by an absorption technique, but the dynamic range of this technique is rather narrow. In addition, SiH_4 is not transparent at 121.6 nm.[20,21] The dynamic range of the two-photon LIF technique is wide, but only relative values can be obtained. By combining these two techniques, it is possible to determine the absolute densities under various conditions.

In the two-photon LIF measurements, the output of a dye laser (Lumonics HD-500) pumped by a YAG (Y/Al garnet) laser (Spectra Physics PRO-190) at 615.3 nm was tripled in frequency by using two BBO (β-BaB_2O_4) crystals and a polarization rotator (Solar). This tripling procedure is the same as that reported elsewhere.[22] The third-harmonic wavelength, 205.1 nm, corresponds to the transitions to the $3s\,^2S_{1/2}$, $3d\,^2D_{3/2}$, and $3d\,^2D_{5/2}$ states from the ground $1s\,^2S_{1/2}$ state. A Pellin Broca prism (Sigma Koki) was used to separate the third harmonic from the second harmonic and the fundamental. The laser beam was focused with a 400-mm focal-length lens (Sigma Koki). Emissions corresponding to the $3s\,^2S$-$2s\,^2P$ and $3d\,^2D$-$2s\,^2P$ transitions around 656.3 nm (Balmer α) were collected through a 350-mm focal-length plano-convex collimating lens (Sigma Koki) and a 150-mm focal-length biconvex focusing lens (Sigma Koki) and detected with a photomultiplier tube (Hamamatsu Photonics R212UH). A slit and a cutoff filter (Hoya R62), which eliminates the emissions below 600 nm, were inserted between the focusing lens and the photomultiplier tube to reduce the stray light and the blackbody radiation from the catalyzer. The LIF signal was recorded with a boxcar averager-gated integrator system (Stanford Research Systems SR240/SR250/SR280) or a digital oscilloscope (LeCroy 9310CM). The inner side of the quartz window for Balmer α observation was coated with nonvolatile oil to prevent the light-scattering caused by film deposition. The typical pulse energy of the laser was 0.6 mJ. Below this energy, the LIF intensity increased quadratically with increases in the pulse energy.

In the vacuum ultraviolet absorption measurements, the output of the dye laser at 729.6 nm was doubled in frequency by a BBO crystal (Solar) and then tripled by a mixture of Kr and Ar to produce Lyman α light at 121.6 nm.[23–25] The typical pressures of Kr and Ar were 13 and 53 kPa, respectively, while the laser-pulse energy at 364.8 nm was 8 mJ. The 364.8-nm light was focused into the tripling cell, 15 cm in length, by a 150-mm focal-length lens. The 121.6-nm light was collimated with an MgF_2 lens (100-mm focal length at 121.6 nm). After passing through the CVD chamber, the laser beam entered a detection vessel filled with 130 Pa of NO. The NO^+ ions produced were collected by parallel electrodes, and the ion current was measured with a boxcar averager-gated integrator system (Stanford Research Systems SR240/SR250/SR280). The ion current is proportional to the vacuum ultraviolet intensity when appropriate voltage is applied.[26–28] The typical dc voltage applied to the electrodes was +200 V. There was no change in the absorption spectral profiles when the NO pressure was changed by a factor of 2 or the dc voltage was changed by ± 100 V. The absorption profile also depended little on the laser intensity. Of course, no ion current was observed in the absence of Kr. A schematic diagram of the experimental apparatus is shown in Fig. 1.

The transmittance was measured by scanning the frequency of the laser. By simulating the absorption profiles, it is possible to evaluate the absolute densities of H-atoms. Since Lyman α consists of two separated lines, corresponding to the $2p\,^2P_{1/2}$-$1s\,^2S_{1/2}$ and $2p\,^2P_{3/2}$-$1s\,^2S_{1/2}$ transitions, the transmittance is given by:[29]

$$\frac{\int_{-\infty}^{\infty}\exp\left\{-\left(\frac{\nu-\nu_L}{\alpha}\right)^2\right\}\exp\left\{-k_1 l\exp\left(-\left(\frac{\nu-\nu_1}{\beta_1}\right)^2\right)-k_0 l\exp\left(-\left(\frac{\nu-\nu_0}{\beta_0}\right)^2\right)\right\}d\nu}{\int_{-\infty}^{\infty}\exp\left\{-\left(\frac{\nu-\nu_L}{\alpha}\right)^2\right\}d\nu}.$$

Here, both the spectral profiles of the light source and the absorbing media were assumed to be Gaussian, and the Lorentz broadening was ignored. The values of α, β_0, and β_1 represent the bandwidths of the laser and H-atom absorption spectra, ν_0 and ν_1 are the frequencies at the absorption peaks, ν_L is the central frequency of the laser, k_0 and k_1 are the absorption coefficients at the Doppler-broadened line centers, and l is the absorption path length, 45 cm in the present system. The values of β_0, β_1, k_0, and k_1 are given by:

$$\beta_0=\left(\frac{2kT}{m}\right)^{1/2}\frac{\nu_0}{c},$$

$$\beta_1=\left(\frac{2kT}{m}\right)^{1/2}\frac{\nu_1}{c},$$

$$k_0=\left(\frac{m}{2\pi kT}\right)^{1/2}\frac{c^3N}{8\pi\tau\nu_0^3},$$

$$k_1=\left(\frac{m}{2\pi kT}\right)^{1/2}\frac{c^3N}{4\pi\tau\nu_1^3},$$

where m is the mass of H atoms, k is the Boltzmann constant, T is the absolute translational temperature, c is the speed of light, N is the density of ground-state H-atoms, and τ is the radiative lifetime of $H(2p\,^2P_J)$, 1.60 ns.

SiH_4 (Takachiho 99.9999%), H_2 (Takachiho 99.99995%), Kr (Nihon Sanso 99.995%), Ar (Nihon Sanso 99.9995%), and NO (Nihon Sanso 99%) were used from cylinders without further purification.

III. RESULTS

A. Two-photon laser-induced fluorescence (LIF) measurements

When the catalyzer was heated to higher than 1300 K in the presence of more than 2 Pa of H_2, it was possible to detect H-atoms by two-photon LIF. No LIF signal was observed when the catalyzer was not heated. This was true even in the presence of SiH_4. In other words, two-photon dissociation of H_2 or SiH_4 to produce H-atoms can be ignored. The production of H-atoms by the photodissociation of Si_2H_6, which can be produced in the SiH_3+SiH_3 reaction, has been demonstrated by Miyazaki *et al.*[30] However, the steady-state density of Si_2H_6 in our system is more than one order of magnitude smaller than that of SiH_4.[6] In the present measurements, the SiH_4 density was less than 2×10^{13} cm^{-3}, which is on the same order as that of H-atoms observed. If Si_2H_6 is produced, that contribution should be minor.

The H-atom density increased in proportion to the square root of the H_2 pressure below 7 Pa, as shown in Fig. 2, suggesting that there is a thermal equilibration between H_2 and H on the catalyzer surfaces. The absolute values of the H-atom densities in Fig. 2 were determined by a vacuum ultraviolet absorption technique. Figure 3 is a van't Hoff type plot in the presence of pure H_2. In this figure, a logarithm of the H-atom density is plotted as a function of the inverse of the catalyzer temperature. The pressure and flow rate of H_2 were 5.6 Pa and 150 sccm, respectively. The slope of the linear plot in Fig. 3 represents the effective enthalpy for the H-atom formation from H_2 on the catalyzer surfaces, which was determined to be 239 kJ mol^{-1}. This value is in fair agreement with the literature values obtained using Ta and Re as catalyzers, 237 and ~230 kJ mol^{-1}, respectively.[11] These values are also similar to those obtained from the equilibrium constant in the gas phase, 228 kJ mol^{-1},[11] suggesting that the H–H bond scission is rate-determining and that this process depends little on the character of the catalyzer. In sharp contrast, in the decomposition of SiH_4, the effective enthalpy for the production of Si atoms depends on

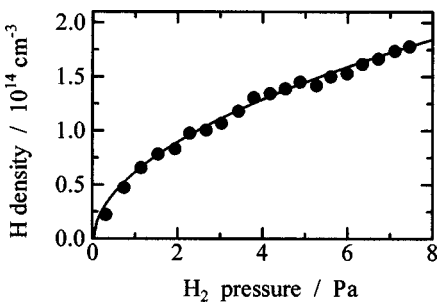

FIG. 2. H_2 pressure dependence of the H-atom density measured by a two-photon laser-induced fluorescence technique. The catalyzer temperature was 2200 K.

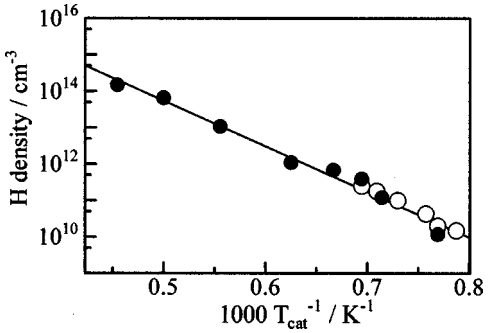

FIG. 3. Catalyzer temperature, (T_{cat}), dependence of the H-atom density between 1270 and 2200 K in the presence of 5.6 Pa of H_2 measured by a two-photon laser-induced fluorescence technique (●) and by a vacuum ultraviolet absorption technique (○). The absolute values were determined by a vacuum ultraviolet absorption technique.

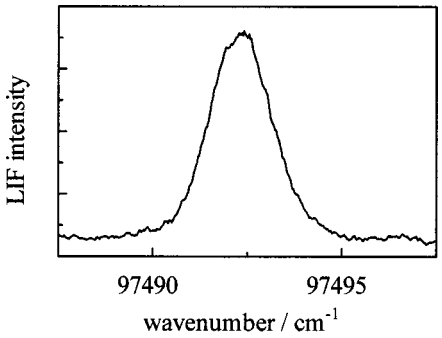

FIG. 4. Doppler profile of H-atoms measured by a two-photon laser-induced fluorescence technique in the presence of 5.6 Pa of pure H_2. The catalyzer temperature was 2200 K.

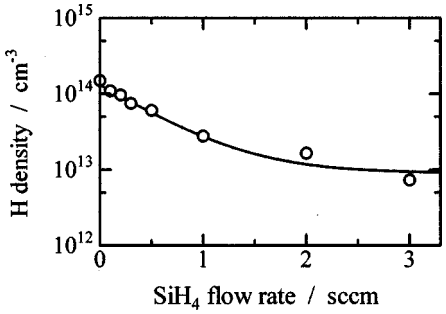

FIG. 5. The dependence of the H-atom density on the SiH_4 flow rate. The pressure and the flow rate of H_2 were 5.6 Pa and 150 sccm, respectively. The catalyzer temperature was 2200 K.

the character of the catalyzer. The effective enthalpies below 1700 K have been measured to be 250, 100, and 70 kJ mol^{-1} for Mo, Ta, and W, respectively.[8] In addition, the effective enthalpies are smaller at higher temperatures.[7,8]

In the above measurements, the wavelength of the laser was fixed at the absorption peak. The translational temperature of H-atoms, and then the absorption spectral profile, may change with the catalyzer temperature. However, this influence is minor. As will be shown below, the translational temperature of H-atoms in the presence of 5.6 Pa of H_2 is as low as 450 ± 60 K when the catalyzer temperature is 2200 K. If the translational temperature decreases down to 300 K when the catalyzer temperature is lowered, the change in the LIF spectral width is just 10% and may be ignored.

Figure 4 shows the Doppler profile of H-atoms measured in the presence of 5.6 Pa of pure H_2. The two-photon LIF signal was recorded as a function of the two-photon energy of the laser in wavenumber units. The catalyzer temperature was 2200 K. From such profiles, the translational temperature of H-atoms can be determined.[29,31,32] The measured LIF spectrum is the superposition of three transitions onto the $3s\,^2S_{1/2}$, $3d\,^2D_{3/2}$, and $3d\,^2D_{5/2}$ states. The spectral separations, 0.098 and 0.036 cm^{-1},[33] are smaller than the expected Doppler width, but cannot be ignored. The Doppler width was evaluated by simulating the measured spectral profiles. The relative transition probabilities for the two-photon $3s$-$1s$ and $3d$-$1s$ transitions have been reported by Goldsmith and Rahn.[34] The laser bandwidth, which is also necessary to simulate the spectrum, was determined experimentally by measuring the Doppler profile of the $2+1$ resonance-enhanced multiphoton ionization signal of Kr at 202.3 nm, which corresponds to the transition to the $4s^24p^5(^2P^*_{1/2})5p$ state. The translational temperature of H-atoms was determined to be 450 ± 60 K, which is consistent with the rotational temperature of SiH obtained under similar conditions, 390 ± 40 K.[6]

By the introduction of SiH_4, the H-atom density decreased sharply. Figure 5 shows the dependence of the H-atom density on the SiH_4 flow rate. The flow rate of H_2 and the catalyzer temperature were kept constant at 150 sccm and 2200 K, respectively. The H-atom density was measured 1 min after the introduction of SiH_4. With low SiH_4 flow rates, such as 0.2 sccm, the H-atom density decreased against time after this period and took ~5 min to level off. At high flow rates such as at 2 sccm, the LIF signal was constant against time, likely leveling off within 1 min. The decrease in H-atom density due to the introduction of SiH_4 cannot be ascribed to the collisional quenching of the upper states, $H(3s\,^2S$ or $3d\,^2D)$, because of their short lifetimes as well as the low concentrations of SiH_4, although the quenching rate constant is expected to be large.[35] The poisoning of the catalyzer surfaces by SiH_4 does not take place when the catalyzer temperature is higher than 1900 K.[1] When the SiH_4 flow was interrupted, the H-atom density recovered slowly, taking ~10 min to increase back to the level before the introduction. During the recovery, it was possible to detect SiH_4 mass-spectrometrically, indicating that SiH_4 is produced by the reaction between H-atoms and the silicon compounds deposited on the chamber walls and the substrates. Details of the mass-spectrometric measurements have been described elsewhere.[6,7]

It was difficult to observe H-atoms in the presence of pure SiH_4 without H_2 dilution. However, this does not necessarily mean that the production of H-atoms from SiH_4 is minor. H-atoms, if produced, should be lost immediately on chamber walls under the present conditions. Under some conditions, polycrystalline silicon films can be fabricated without H_2 dilution,[36] suggesting an efficient production of H-atoms from SiH_4. Tange *et al.* have also succeeded in detecting H-atoms in the catalytic decomposition of SiH_4.[8]

B. Vacuum ultraviolet absorption measurements

By measuring the absorption of Lyman α light, it is possible to determine the absolute densities of H-atoms. If the absolute density is determined in the pure H_2 system, the relative values obtained by two-photon LIF can be put on an absolute scale. When the catalyzer temperature was 2200 K, the transmittance of the vacuum ultraviolet radiation at 121.6 nm in the presence of 5.6 Pa of H_2 was too low to be measured quantitatively. For quantitative measurements, it was necessary to lower the catalyzer temperature to 1410 K. Figure 6 shows the absorption spectra at four catalyzer temperatures, 1270, 1320, 1370, and 1410 K. The flow rate and the pressure of H_2 were 150 sccm and 5.6 Pa, respectively.

From the absorption spectra shown in Fig. 6, the absolute densities of H-atoms can be determined by fitting the experimentally observed spectra with the simulated ones. The translational temperature, T, the bandwidth of the

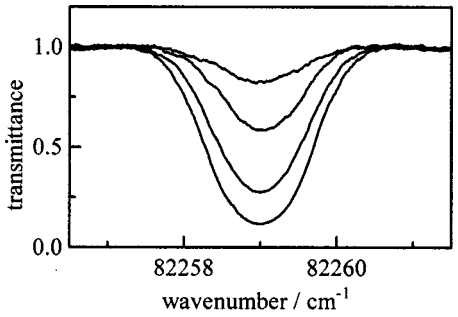

FIG. 6. Vacuum ultraviolet absorption spectra of H-atoms. The catalyzer temperatures were 1270, 1320, 1370, and 1410 K from top to bottom. The pressure and the flow rate of H_2 were 5.6 Pa and 150 sccm, respectively.

vacuum ultraviolet laser, α, and the absolute density of H-atoms, N, were parametrized. The best fit was obtained when T and α were assumed to be 300 K and 0.7 cm^{-1}, respectively. The minimum transmittance depended little on the choice of these parameters and was primarily determined by the atomic density, N. The estimated uncertainty in the translational temperature is ± 60 K, although the translational temperature lower than room temperature cannot be expected. The catalyzer-temperature dependence of the H-atom density is shown in Fig. 3 together with that obtained by two-photon LIF measurements.

IV. DISCUSSION

The sharp decrease in the H-atom density with increases in the flow rate of SiH_4 should result from the reaction with silicon compounds deposited on the chamber walls. There may be some contribution of gas-phase reactions, but this contribution is minor. When the flow rate is 3 sccm, the SiH_4 pressure is 0.11 Pa, which corresponds to the density of 1.8×10^{13} cm^{-3} at 450 K. With the addition of this amount of SiH_4, the H-atom density decreased from 1.5×10^{14} cm^{-3} to 7.0×10^{12} cm^{-3}. In other words, one SiH_4 molecule consumed eight hydrogen atoms, a result that cannot be explained by gas-phase reactions. In contrast, if H-atoms are removed on surfaces, the following chain reactions are expected:

$$H + SiH_4 \rightarrow H_2 + SiH_3,$$

$$SiH_3 \rightarrow a\text{-Si:H},$$

$$a\text{-Si:H} + H \rightarrow SiH_4.$$

With the introduction of SiH_4, even 0.2 sccm, silicon compounds must deposit on the chamber walls, drastically increasing the surface-loss probability. The slow decrease in the H-atom density when 0.2 sccm of SiH_4 was introduced is consistent with this model. At such a small flow rate, it takes a long time to cover the chamber walls with silicon compounds.

A similar decrease in the H-atom density has been observed in plasma-enhanced CVD processes.[37] Kae-Nune *et al.* have shown that in a parallel-plate radio-frequency discharge of H_2, the H-atom density decreases from 2.5×10^{12} cm^{-3} to 2×10^{11} cm^{-3} when 0.4 Pa of SiH_4 is added to 40 Pa of H_2.[37] This change has also been attributed to a change in the surface-loss probabilities of H-atoms. The decay profiles of H-atom densities after pulsed discharges were also measured and the absolute surface-loss probabilities were determined. The probability on stainless steel was determined to be 0.2 ± 0.05, while that on amorphous silicon during the deposition was found to be almost unity.[37] The loss probability of H-atoms on stainless steel surfaces reported by Tserepi and Miller is smaller, ~0.04.[38] When the surface is covered with some inert species, the surface-loss probability can be even smaller, $0.01\sim0.001$.[39] In our present system, the chamber wall may be partially coated with SiN_x,

TABLE I. Comparison of the H-atom densities in plasma-enhanced CVD and catalytic CVD processes.

Gas pressure	Production procedure	Detection procedure	Density / cm^{-3}	Reference
H_2 230 Pa	dc	VUV LIF	$10^{10}\sim10^{13}$	Kajiwara (Ref. 45)
H_2 400 Pa	rf 10 W	2 photon LIF Titration	8×10^{13}	Tserepi (Ref. 46)
SiH_4 2.0 Pa	rf 20 W	2 photon LIF	3×10^{11}	Park (Ref. 47)
H_2 130 Pa	dc 20–50 mA	2 photon LIF VUV absorption	1.3×10^{13}	Amorim (Ref. 48)
H_2 13 Pa	rf 100 W	2 photon LIF VUV absorption	6×10^{12}	Tachibana (Ref. 19)
SiH_4 13 Pa	rf 5 W	2 photon LIF VUV absorption	4×10^{12}	Tachibana (Ref. 19)
H_2+10%SiH_4 13 Pa	rf 2 W	2 photon LIF VUV absorption	4×10^{11}	Tachibana (Ref. 19)
H_2 40 Pa	rf 50 W	Mass spectrom.	2.5×10^{12}	Kae-Nune (Ref. 37)
H_2+1%SiH_4 40 Pa	rf 50 W	Mass spectrom.	2×10^{11}	Kae-Nune (Ref. 37)
SiH_4 11 Pa	rf 2 W	2 photon LIF Titration	5×10^{11}	Miyazaki (Ref. 49)
H_2 5.6 Pa	Catalysis 2200 K	2 photon LIF VUV absorption	1.5×10^{14}	present
H_2+2%SiH_4 5.6 Pa	Catalysis 2200 K	2 photon LIF VUV absorption	7×10^{12}	present

since we have used this chamber to deposit SiN_x by using an NH_3/SiH_4 mixture. SiN_x may be inert against the surface recombination of H-atoms.

Table I compares the H-atom densities in the gas phase measured in the present work with those obtained in plasma-enhanced CVD processes. The H-atom density in the Cat-CVD apparatus is more than one order of magnitude larger than that in the standard plasma-enhanced CVD apparatus, although quantitative comparison is difficult because the absolute densities may strongly depend on the wall conditions.

The characteristic high density of H-atoms in the Cat-CVD apparatus should open many application fields for processing, not only for deposition but also for etching, chamber cleaning, annealing, and structural modification.[15–17,40–43] The etching rate of crystalline silicon by H-atoms produced by catalytic decomposition is as large as 3.8 $nm\,s^{-1}$ when the silicon surface temperature is low, ~350 K.[15–17] By utilizing the silicon hydride species generated in this etching process, Kamesaki *et al.* have recently succeeded in producing a large grain-size (exceeding 1 μm) polycrystalline silicon film.[16,17] H-atoms can also be used for *in situ* chamber cleaning. Chamber cleaning without the use of halogen compounds is desirable from an environmental as well as an economical point of view. The etching rate decreases with increases in the surface temperature.[16,17] Then, it is desirable to heat the chamber walls during deposition and to cool during cleaning. Crystallization of amorphous silicon by H-atoms (atomic hydrogen anneal) also takes place efficiently.[40,41] The crystalline fraction of silicon films increases from 0 to several tens percent by this treatment. H-atoms produced by the present technique can also be used for the surface cleaning or structural modification of GaAs[42] and SiN_x.[43] When GaAs surfaces are exposed to the catalytic decomposition products of H_2 or NH_3, the oxygen related peaks on the x-ray photoelectron spectra are reduced.[42] By the post-deposition treatment, the leakage current of SiN_x films is lowered by three orders of magnitude.[43] H-atoms must play major roles in such modification processes. Of course, similar treatments may be possible by using plasma, but the catalytic process is superior because of its high decomposition efficiency.

There may be problems caused by the abundance of a large amount of H-atoms in Cat-CVD. For example, transparent conducting oxide materials such as SnO_2, which is widely used in solar cells, should be reduced to metallic Sn by H-atoms. In such cases, the transmittance in the visible region should decrease. However, under practical deposition conditions, the deposition of *a*-Si:H is faster than the reduction process, and no problems occur.[44] In addition, reduction can be avoided by coating SnO_2 with ZnO.[44]

V. CONCLUSIONS

H-atoms are efficiently produced in catalytic decomposition of H_2 on heated W surfaces. The density of H-atoms is one or two orders of magnitude higher than the densities observed in typical plasma-enhanced CVD processes. The H-atom density decreases sharply with the addition of SiH_4. This decrease appears to primarily be due to the reaction with silicon compounds deposited on chamber walls. In other words, the radical densities in the gas phase strongly depend on the wall conditions. The characteristic high density of H-atoms will likely open many application fields for processing, including etching, chamber cleaning, annealing, and structural modification processes.

ACKNOWLEDGMENTS

This work is in part supported by the R & D Projects in Cooperation with Academic Institutions ''Cat-CVD Fabrication Processes for Semiconductor Devices'' entrusted from the New Energy and Industrial Technology Development Organization (NEDO) to the Ishikawa Sunrise Industries Creation Organization (ISICO) and carried out at Japan Advanced Institute of Science and Technology (JAIST).

[1] H. Matsumura, Jpn. J. Appl. Phys., Part 1 **37**, 3175 (1998).
[2] H. Matsumura, Jpn. J. Appl. Phys., Part 2 **25**, L949 (1986).
[3] J. Doyle, R. Robertson, G. H. Lin, M. Z. He, and A. Gallagher, J. Appl. Phys. **64**, 3215 (1988).
[4] A. H. Mahan, J. Carapella, B. P. Nelson, R. S. Crandall, and I. Balberg, J. Appl. Phys. **69**, 6728 (1991).
[5] R. E. I. Schropp, K. F. Feenstra, E. C. Molenbroek, H. Meiling, and J. K. Rath, Philos. Mag. B **76**, 309 (1997).
[6] Y. Nozaki, K. Kongo, T. Miyazaki, M. Kitazoe, K. Horii, H. Umemoto, A. Masuda, and H. Matsumura, J. Appl. Phys. **88**, 5437 (2000).
[7] Y. Nozaki, M. Kitazoe, K. Horii, H. Umemoto, A. Masuda, and H. Matsumura, Thin Solid Films **395**, 47 (2001).
[8] S. Tange, K. Inoue, K. Tonokura, and M. Koshi, Thin Solid Films **395**, 42 (2001).
[9] H. L. Duan, G. A. Zaharias, and S. F. Bent, Thin Solid Films **395**, 36 (2001).
[10] J. N. Smith, Jr. and W. L. Fite, J. Chem. Phys. **37**, 898 (1962).
[11] S. A. Redman, C. Chung, K. N. Rosser, and M. N. R. Ashfold, Phys. Chem. Chem. Phys. **1**, 1415 (1999).
[12] S. K. Loh and J. M. Jasinski, J. Chem. Phys. **95**, 4914 (1991).
[13] N. L. Arthur and L. A. Miles, J. Chem. Soc., Faraday Trans. **93**, 4259 (1997).
[14] N. L. Arthur and L. A. Miles, Chem. Phys. Lett. **282**, 192 (1998).
[15] A. Izumi, H. Sato, S. Hashioka, M. Kudo, and H. Matsumura, Microelectron. Eng. **51-52**, 495 (2000).
[16] K. Kamesaki, A. Masuda, A. Izumi, and H. Matsumura, Thin Solid Films **395**, 169 (2001).
[17] H. Matsumura, K. Kamesaki, A. Masuda, and A. Izumi, Jpn. J. Appl. Phys., Part 2 **40**, L289 (2001).
[18] J. Bokor, R. R. Freeman, J. C. White, and R. H. Storz, Phys. Rev. A **24**, 612 (1981).
[19] K. Tachibana, Jpn. J. Appl. Phys., Part 1 **33**, 4329 (1994).
[20] M. Suto and L. C. Lee, J. Chem. Phys. **84**, 1160 (1986).
[21] U. Itoh, Y. Toyoshima, H. Onuki, N. Washida, and T. Ibuki, J. Chem. Phys. **85**, 4867 (1986).
[22] H. Umemoto, Chem. Phys. Lett. **314**, 267 (1999).
[23] R. Mahon, T. J. McIlrath, and D. W. Koopman, Appl. Phys. Lett. **33**, 305 (1978).
[24] R. Wallenstein, Opt. Commun. **33**, 119 (1980).
[25] R. Hilbig and R. Wallenstein, IEEE J. Quantum Electron. **QE-17**, 1566 (1981).
[26] K. Watanabe, J. Chem. Phys. **22**, 1564 (1954).
[27] T. Masuoka and T. Oshio, Jpn. J. Appl. Phys., Part 1 **15**, 65 (1976).
[28] A. L. Di Domenico, C. Graetzel, and J. L. Franklin, Int. J. Mass Spectrom. Ion Phys. **33**, 349 (1980).
[29] A. C. G. Mitchell and M. W. Zemansky, *Resonance Radiation and Excited Atoms* (Cambridge University Press, London, 1934).
[30] K. Miyazaki, T. Kajiwara, K. Uchino, K. Muraoka, T. Okada, and M. Maeda, J. Vac. Sci. Technol. A **14**, 125 (1996).
[31] H. Umemoto, T. Nakae, H. Hashimoto, K. Kongo, and M. Kawasaki, J. Chem. Phys. **109**, 5844 (1998).

[32] H. Umemoto, T. Asai, H. Hashimoto, and T. Nakae, J. Phys. Chem. A **103**, 700 (1999).
[33] NIST Database for Atomic Spectroscopy.
[34] J. E. M. Goldsmith and L. A. Rahn, Opt. Lett. **15**, 814 (1990).
[35] J. Bittner, K. Kohse-Höinghaus, U. Meier, and Th. Just, Chem. Phys. Lett. **143**, 571 (1988).
[36] M. Ichikawa, J. Takeshita, A. Yamada, and M. Konagai, Jpn. J. Appl. Phys., Part 2 **38**, L24 (1999).
[37] P. Kae-Nune, J. Perrin, J. Jolly, and J. Guillon, Surf. Sci. **360**, L495 (1996).
[38] A. D. Tserepi and T. A. Miller, J. Appl. Phys. **75**, 7231 (1994).
[39] M. A. Childs, K. L. Menningen, L. W. Anderson, and J. E. Lawler, J. Chem. Phys. **104**, 9111 (1996).
[40] A. Heya, A. Masuda, and H. Matsumura, Appl. Phys. Lett. **74**, 2143 (1999).
[41] A. Heya, A. Masuda, and H. Matsumura, J. Non-Cryst. Solids **266-269**, 619 (2000).
[42] A. Izumi, A. Masuda, S. Okada, and H. Matsumura, Inst. Phys. Conf. Ser., Bristol, 1997, No. 155, p. 343.
[43] H. Sato, A. Izumi, and H. Matsumura, Appl. Phys. Lett. **77**, 2752 (2000).
[44] K. Imamori, A. Masuda, and H. Matsumura, Thin Solid Films **395**, 147 (2001).
[45] T. Kajiwara, M. Inoue, T. Okada, K. Muraoka, M. Akazaki, and M. Maeda, Rev. Sci. Instrum. **56**, 2213 (1985).
[46] A. D. Tserepi, J. R. Dunlop, B. L. Preppernau, and T. A. Miller, J. Appl. Phys. **72**, 2638 (1992).
[47] W. Z. Park, M. Tanigawa, T. Kajiwara, K. Muraoka, M. Masuda, T. Okada, M. Maeda, A. Suzuki, and A. Matsuda, Jpn. J. Appl. Phys., Part 1 **31**, 2917 (1992).
[48] J. Amorim, G. Baravian, M. Touzeau, and J. Jolly, J. Appl. Phys. **76**, 1487 (1994).
[49] K. Miyazaki, T. Kajiwara, K. Uchino, K. Muraoka, T. Okada, and M. Maeda, J. Vac. Sci. Technol. A **15**, 149 (1997).